

# Floating Models for 3D Building Modeling from Topographic Maps and LiDAR Data

Sendo Wang<sup>1</sup>, Yi-Hsing Tseng<sup>2</sup> and Ayman F. Habib<sup>3</sup>

<sup>1</sup> Post-doctoral Research Fellow, Department of Geomatics Engineering, University of Calgary, 2500 University Drive N.W., Calgary, Alberta, Canada T2N 1N4, [sendo@ucalgary.ca](mailto:sendo@ucalgary.ca)

<sup>2</sup> Professor, Department of Geomatics, National Cheng Kung University, 1 University Road, Tainan City, Taiwan 70101, [tseng@mail.ncku.edu.tw](mailto:tseng@mail.ncku.edu.tw)

<sup>3</sup> Professor, Department of Geomatics Engineering, University of Calgary, 2500 University Drive N.W., Calgary, Alberta, Canada T2N 1N4, [ahabib@ucalgary.ca](mailto:ahabib@ucalgary.ca)

## ABSTRACT

A novel approach of *Model-based Building Reconstruction* (MBBR) from topographic maps and LiDAR data called *Floating Models* is proposed in this paper. Floating models are a series of pre-defined primitive models which are floating in the space. Its size is adjustable by shape parameters, while its location and rotation is controlled by pose parameters. A building is reconstructed by adjusting these model parameters so the wire-frame model adequately fits into the building's outlines among the topographic maps, LiDAR data and DEM. This model-based reconstruction provides good constraints to the shape of the model in contrary to the data-based approach. In this paper, the model parameters are re-arranged into two groups: horizontal and vertical parameters. The horizontal parameters are determined by fitting the top or bottom boundary of the model to the topographic maps. The vertical parameters are decided by fitting the top surface of the model to the LiDAR data and interpolating the datum point's height from DEM. To achieve a balance between accuracy and efficiency, a semi-automated reconstruction procedure is proposed. First, the computer will automatically generate all building models with polygonal prism models from maps and LiDAR data. Second, the operator may click a model and change it to a box or gable-roof model, and approximately fit to the building's outlines on the topographic map. Third, the computer calculates the optimal fit between the model and the topographic map based on an *ad hoc* least-squares model fitting algorithm. Fourth, the computer calculates the roof or ridge height from the LiDAR points within the roof's boundary. Finally, the model parameters and standard deviations are provided, and the wire-frame model is superimposed on all overlapped aerial photos for manual final-check. The operator can make any necessary modification by adjusting the corresponding model parameter. A 528hectare urban area in Taipei City is reconstructed for testing. The fitting result is compared to the manually photogrammetric reconstruction result. Most of modern buildings can be completely modeled, and fitting result achieves the photogrammetric accuracy.

**Keywords:** Building, Reconstruction, LiDAR, Photogrammetry, Digital City Model

## 1 INTRODUCTION

In response to the development of 3D City Spatial Information Systems for urban planning and management, acquisition of 3D data of city objects has increasingly become an important topic (Braun *et al.*, 1995; Englert and Gülch, 1996; Grün, 2000; Lang and Förstner, 1996; Vosselman and Veldhuis, 1999). Conventional photogrammetry concentrates on the accurate 3D coordinate measurement of points. The automated measuring systems set up by image matching algorithms are still based on the point-to-point correspondence. However, higher-order features such as linear, planar or volumetric features contain much more geometric and semantic information than a single point. That encourages many researches toward using 3D CAD models as a modeling tool to extracting objects from source data (Bhanu *et al.*, 1997; Böhm *et al.*, 2000; Brenner, 2000; Das *et al.*, 1997; Ermes, 2000; Tseng and Wang, 2003; van den Heuvel, 2000). This trend towards integration of photogrammetry and CAD system in the algorithmic aspect creates a new term: "*CAD-based Photogrammetry*". Researches show that using CAD models does increase the efficiency of photogrammetric modeling both by the advanced object modeling techniques, such as *Constructive Solid Geometry* (CSG), and the incorporation of geometric object constraints.

Inspired by the CAD-based photogrammetry, we propose a novel measuring tool – *Floating Models* – for reconstructing building from both 2D and 3D data. The floating model represents a flexible entity floating in the 3D space. It can be a point, a line segment, a surface plane, or a volumetric model. Each model is associated with a set

of shape parameters and a set of pose parameters. The pose parameters determine the datum point's position and the orientation of the model. The shape parameters change the model's outline and volume. From the traditional photogrammetric point of view, the floating models are extension of the floating mark. However, compare to the floating mark, the floating model does not only float in the object space, but also can be deformed to fit the outline of the object. From the model-based building reconstruction's point of view, floating mark is an exceptional case of floating models without any shape parameter.

Model-based building reconstruction starts with hypotheses of building model representing a specified target on the scene, and verifies the compatibility between the model and the existing data, such as topographic maps, aerial photos, LiDAR data, and DEM (Ameri, 2000; Brenner, 1999; Sester and Förstner, 1989; Wang and Tseng, 2008). Most of the MBBR approaches are implemented in a semi-automatic manner, solving the model-data fitting problem based on some high-level information given by the operator. While the model-data fitting is optimally achieved, the spatial parameters of a building model are determined. Therefore, the key is the algorithm that is able to determine the pose and shape parameters of a floating model such that the edge segments of the wire-frame are optimally aligned with the corresponding edge elements from multiple data sources. To deal with this problem, we propose a tailored *Least-squares Model-data Fitting* (LSMDF) algorithm as a major component of the building reconstruction framework.

To simplify the fitting problem, the model parameters are rearranged into two groups, horizontal and vertical parameters. Hence the model-data fitting procedures are also divided into three steps. First, fit model to topographic maps to derive horizontal parameters. Second, interpolate datum's height from DEM and fit model to LiDAR data to derive vertical parameters. Finally, the wireframe model is projected onto aerial photos for examining. The operator can make further modification of the model according to the photos if necessary. Figure 1 uses a box model as an example to depict the proposed reconstruction procedures. The hexagons depict the information required from the data sources. The parameters labeled in red color are the varied ones during the procedure.

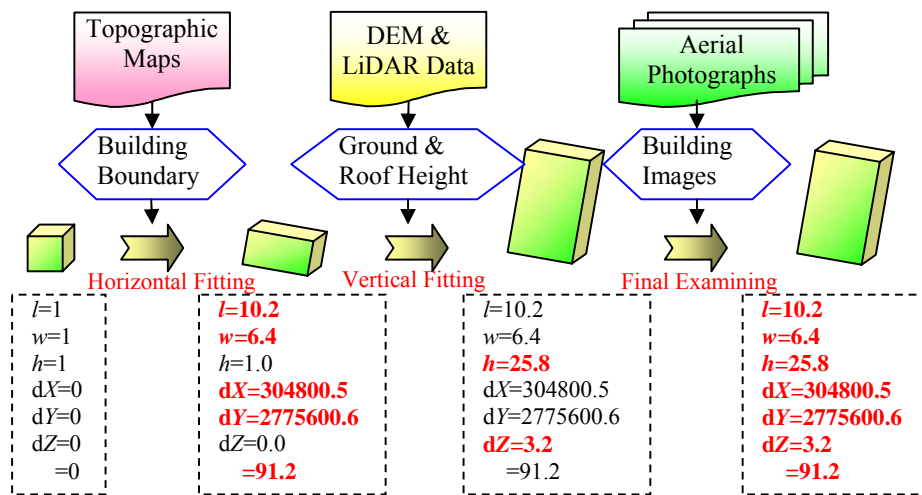


Figure 1. The versatile data sources and the flowchart of the reconstructing procedures.

## 2 FLOATING MODELS

Conventional photogrammetric mapping systems concentrate on the accurate measurement of 3D points. The floating mark is a simple way to represent the position of a point in the space, and thus, has been utilized as the only measuring tool on the stereo plotters up to nowadays. However, the floating mark reaches its limits when the conjugate points can not be identified due to the occlusion or the shadow from other obstacles. With the increasing demands of 3D object models, this point-by-point procedure has become the bottleneck in production. To deal with the problem, we propose floating models which complies with the constructive solid geometry. Each floating model is basically a primitive model, which determines the intrinsic geometric property of a part of building. The primitive model could be any kind of practical models as long as it can be defined and represented by parameters. For example, it could be line segment, rectangle, circle, triangle, box, or gable-roof house, etc. Despite the variety in their shape, each primitive model commonly has a datum point, and is associated with a set of pose parameters and a

set of shape parameters. The datum point and the pose parameter determine the position and pose of the floating model in object space. It is adequate to use 3 translation parameters ( $dX$ ,  $dY$ ,  $dZ$ ) to represent the position and 3 rotation parameters, tilt ( $t$ ) around  $Y$ -axis, swing ( $s$ ) around  $X$ -axis, and azimuth ( $\alpha$ ) around  $Z$ -axis to represent the rotation of a primitive model. The shape parameters describe the shape and size of the primitive model, e.g., a box has three shape parameters: width ( $w$ ), length ( $l$ ), and height ( $h$ ). Changing the values of shape parameters elongates the primitive in the three dimensions, but still keeps its shape as a rectangular box. Various primitive may be associated with different shape parameters, e.g., a gable-roof house primitive has an additional shape parameter – roof’s height ( $rh$ ). Figure 2 shows the topology and the model parameters of a box model, a gable-roof model, and a polygonal prism model. The  $X'$ - $Y'$ - $Z'$  coordinate system defines the model space and the  $X$ - $Y$ - $Z$  coordinate system defines the object space. The little pink sphere indicates the datum point of the model. The yellow primitive model is in the original position and pose, while the grey model depicts the position and pose after adjusting parameters. It is very clear that, the model is “floating” in the space by controlling these pose parameters, and the volume is flexible with certain constraints by controlling the shape parameters.

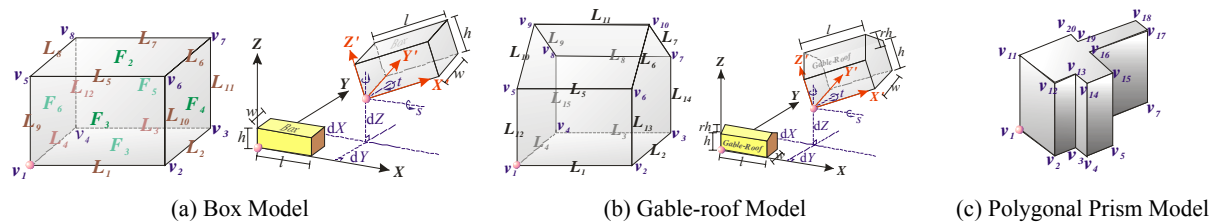


Figure 2. Topology and the model parameters of floating models.

### 3 LEAST-SQUARES MODEL-DATA FITTING

Since the topographic maps are plotted by photogrammetric means, its horizontal accuracy would be better than the LiDAR points cloud. On the contrary, the LiDAR point cloud and DEM provide better vertical accuracy. Therefore, the proposed model-data fitting procedures are separated into two steps: (1) the horizontal parameters are derived by fitting model’s bottom to the topographic map; (2) the vertical parameters are derived by fitting model’s roof to the LiDAR data.

#### 3.1 Horizontal Fitting

The objective of the horizontal fitting is the building’s boundary on the topographic map. However, the map contains much more elements than building boundaries. A “clean & build” process is necessary to erase elements not belong to any building and to establish the close-and-complete polygons instead of poly-lines. These pre-processed polygons are the bases of horizontal fitting. The operator selects an appropriate primitive model and adjusts it to approximately fit to the corresponding polygon. The polygon’s boundary is then re-sampled as sample points with fixed interval. Each sample point would be treated as an observation in the LSMDF to solve the horizontal parameters as optimal fit. Figure 3 depicts the flowchart of the horizontal fitting.

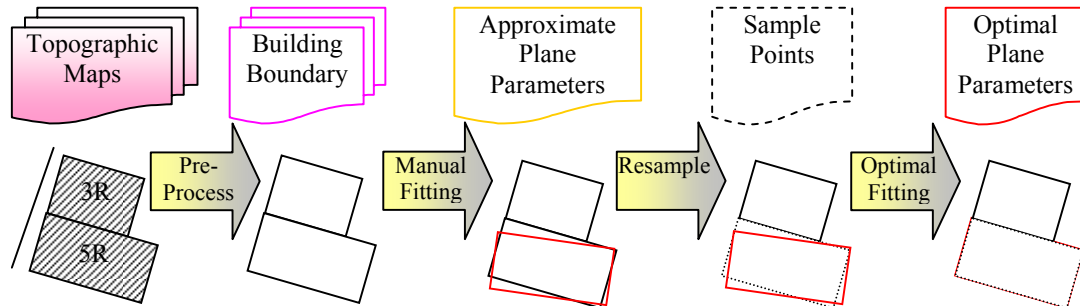


Figure 3. The flowchart of the horizontal fitting.

Since the model has been manually fit, the bottom edges of the wireframe model should be close to the building’s boundary on the map. The approximate horizontal parameters are taken as the initial values, so the LSMDF could iteratively pull the model to the optimal fit instead of blindly search for the solution. A specified buffer zone is set up to filter out irrelevant sample points. Figure 4 depicts the sample point  $T_{ij}$  and the  $w_{buffer}$ -wide buffer determined by an edge  $\overline{v_m v_n}$  of the model. The suffix  $i$  is the index of edge line  $L_i$ , and  $j$  is the index of sample

points. Filtering edge pixels with buffer is reasonable, because the discrepancies between the bottom edges and the corresponding sample points should be small when the model has been fit approximately.

The optimal fitting condition we are looking for is that the edges are exactly falling on the building boundary. In Equation (1), the distance  $d_{ij}$  represents a discrepancy between a sample point  $T_{ij}$  and its corresponding edge  $\overline{v_m v_n}$ , which is expected to be zero. Therefore, the objective of the fitting function is to minimize the squares sum of  $d_{ij}$ . Suppose an edge is composed of the vertices  $v_m(x_m, y_m)$  and  $v_n(x_n, y_n)$ , and there is an edge pixel  $T_{ij}(x_{ij}, y_{ij})$  located inside the buffer. The distance  $d_{ij}$  from the point  $T_{ij}$  to the edge  $\overline{v_m v_n}$  can be formulated as the following equation:

$$d_{ij} = \frac{|(y_m - y_n)x_{ij} + (x_n - x_m)y_{ij} + (y_n x_m - y_m x_n)|}{\sqrt{(x_m - x_n)^2 + (y_m - y_n)^2}} \quad (1)$$

The coordinates of vertices  $v_m(x_m, y_m)$  and  $v_n(x_n, y_n)$  are functions of the unknown horizontal parameters. Therefore,  $d_{ij}$  will be a function of the horizontal parameters. Taking a box model for instance,  $d_{ij}$  will be a function of  $w, l, \alpha, dX$ , and  $dY$ , with the hypothesis that a normal building rarely has a tilt ( $t$ ) or a swing ( $s$ ) angle. The least-squares solution for the unknown parameters can be expressed as:

$$\Sigma d_{ij}^2 = \Sigma [F_{ij}(w, l, \alpha, dX, dY)]^2 \rightarrow \min. \quad (2)$$

Equation (2) is a nonlinear function with regard to the unknowns, so that the Newton's method is applied to solve for the unknowns. The nonlinear function is differentiated with respect to the unknowns and becomes a linear function with regard to the increments of the unknowns as follows:

$$0 + v_{ij} = \left(\frac{\partial F_{ij}}{\partial l}\right)_0 \Delta l + \left(\frac{\partial F_{ij}}{\partial w}\right)_0 \Delta w + \left(\frac{\partial F_{ij}}{\partial dX}\right)_0 \Delta dX + \left(\frac{\partial F_{ij}}{\partial dY}\right)_0 \Delta dY + \left(\frac{\partial F_{ij}}{\partial \alpha}\right)_0 \Delta \alpha + F_{ij0} \quad (3)$$

Where  $F_{ij0}$  is the approximation of the function  $F_{ij}$  calculated with given approximations of the unknown parameters. The linearized equations can be expressed as a matrix form:  $\mathbf{V} = \mathbf{A}\mathbf{X} - \mathbf{L}$ , where  $\mathbf{A}$  is the matrix of partial derivatives;  $\mathbf{X}$  is the vector of the increments;  $\mathbf{L}$  is the vector of approximations; and  $\mathbf{V}$  is the vector of residuals. The objective function actually can be expressed as  $q = \mathbf{V}^T \mathbf{V} \rightarrow \min$ . After each iteration,  $\mathbf{X}$  can be solved by the matrix operation:  $\mathbf{X} = (\mathbf{A}^T \mathbf{A})^{-1} \mathbf{A}^T \mathbf{L}$ . The standard deviation of each increment can also be calculated as the accuracy index of the LSMDF.

### 3.2 Vertical Fitting

Most of the relevant researches adopt 3D plane fitting algorithms to determine the roof patches of the model. In this paper, we propose a coordinate transformation approach to simplify the fitting problem from 3D to 2D. Since the horizontal parameters have been determined optimally at the horizontal fitting stage, the location of the datum point and the horizontal range of the building are determined. Therefore, the height of the datum point could be estimated by 4 neighboring DEM grid nodes with the bi-linear interpolation. The building height ( $h$ ) and the roof's height ( $rh$ ) are determined by fitting model to LiDAR points cloud within the horizontal range of the building. For the flat roof model, such as box and polygonal prism, building height ( $h$ ) is estimated by calculating the mode among all of the point's height, as Figure 5 shows. For the gable-roof model, the LiDAR points cloud is transformed to a local coordinate system defined on the lateral side of the building, then the roof eaves are optimally fit to the points in buffer zone, as Figure 6 depicts. With the coordinate transformation, the observation function of the vertical fitting is simplified as the distance from 2D point to edge, similar to the function of the horizontal fitting.

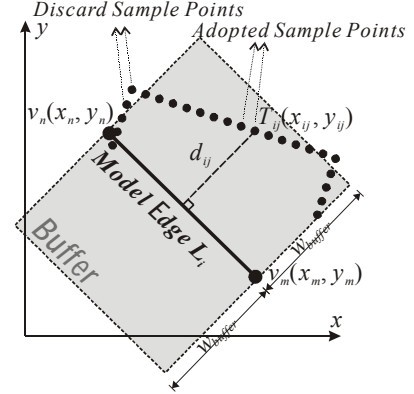


Figure 4. Buffer zone for fitting.

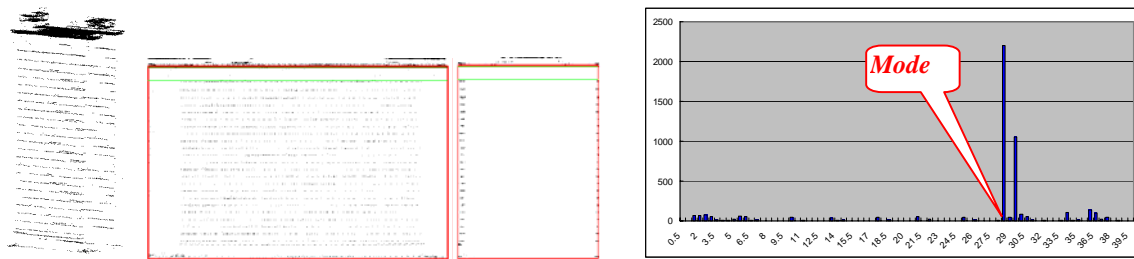


Figure 5. The LiDAR points cloud of a box building and the mode of height among all points.

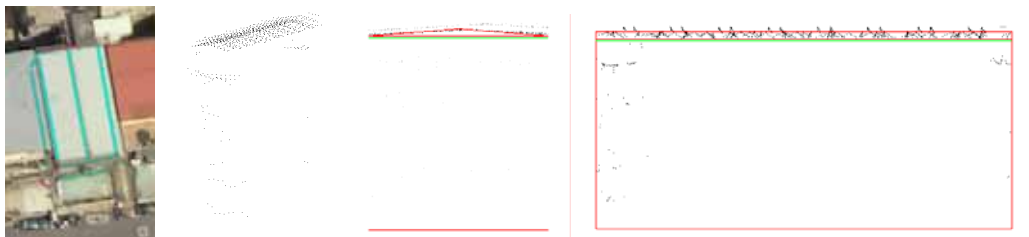


Figure 6. Fitting roof eaves to the LiDAR points cloud in a local coordinate system.

#### 4 EXPERIMENTS

A small urban area of Taipei City about 528hectare is selected for testing the proposed approach. The 1/1000 scale digital topographic maps have been pre-processed to generate building polygons. The grid interval of the corresponding DEM is 4m. The aerial photos are taken by the Vexcel UltraCam D digital photogrammetric camera. The focal length is 101.4mm, the image size is 7500\*11500pixel, and the pixel size is 9 $\mu$ m. The average flight height is about 1930m, so the ground resolution is about 0.17m/pixel. Meanwhile, we develop a PC program by C++ language to implement the proposed building reconstruction procedures. The interface is illustrated by Figure 7. By default, the computer will automatically generate polygonal prism model for all of the buildings on the map by fitting their roofs to LiDAR points cloud. Then, the operator has options to delete or to modify an existing model, or to reconstruct a new model. Whether in the modifying or the reconstructing process, the LSMDF will automatically and optimally fit the model to versatile data sources. In such a semi-automated manner, a building model is usually reconstructed within a minute, but the time for the whole building depends on its complexity. Figure 8 shows the reconstructed 3D models from one sheet of topographic maps.



Figure 7. The interface of the MBBR program.

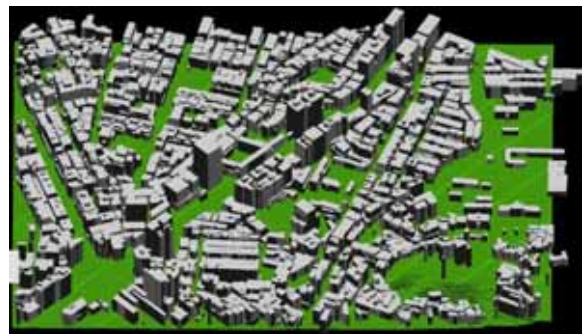


Figure 8. One sheet of reconstructed 3D models.

We select 38 buildings to test the proposed approach and verify the experimental accuracy. They are reconstructed by 217 models, including 94 boxes, 19 gable-roofs, and 104 polygonal-prisms. The coordinates of 634 rooftop vertices are calculated from model parameters as test data (T). Meanwhile, totally 912 vertices measured by experienced photogrammetrist by conventional photogrammetric means as the ground truth (GT). It is assumed as a commission error (C) if there is a vertex reconstructed by MBBR but it's absent in photogrammetric measurement. On the other hand, an omission error (O) is assumed if a vertex measured by photogrammetric means cannot be found in MBBR reconstruction result. Table 1 lists the analysis matrix of correctness and completeness. The 98.26% of the correctness rate proves that MBBR is able to reconstruct the correct vertices of the building roof. But the

31.69% of the omission rate also shows that these three model types are not complete enough to describe the versatile building outlines.

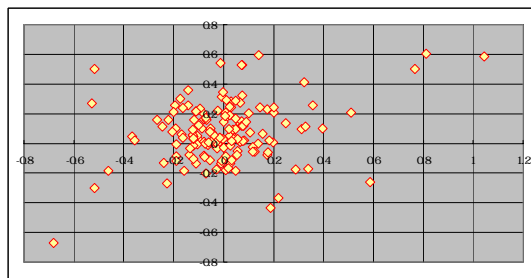
Photogrammetry MBBR	True	False	Total	Commission (C/T)	Correctness (S/T)
True	623(S)	11(C)	634(T)	1.74%	98.26%
False	289(O)		N/A	Omission (O/GT)	Completeness (S/GT)
Total	912(GT)			31.69%	68.31%

**Table 1.** Correctness and completeness analysis.

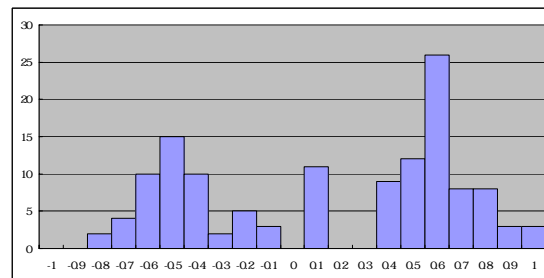
Differences	$\Delta X$	$\Delta Y$	$\Delta Z$
Mean (m)	0.0182	0.0524	0.2563
RMSE (m)	0.2115	0.2028	1.0572

**Table 2.** Statistics of the coordinate differences.

The accuracy of MBBR is evaluated by comparing the 623 successful reconstructed vertices (S) coordinates between MBBR and photogrammetric result. Table 2 lists the statistics of the coordinate differences and Figure 9 shows the distribution of horizontal coordinate differences and the histogram of the vertical height differences. The horizontal coordinate differences are close to a normal distribution and tend to be zero. The RMSE of  $\Delta Z$  shows a large difference between two results. It is due to the inner geometric constraint of the model. For example, the 4 top vertices of a box model would have the same height after reconstructed by MBBR, but their manual stereo measurement would not be exactly the same, especially when there is an annex at one of the corners on the rooftop. Some parapets around the rooftop are not at the same height, too. These outbuildings are the main reasons result in the difference between MBBR and manual photogrammetry.



(a) Horizontal coordinate differences distribution chart.



(b) Vertical height differences histogram.

**Figure 9.** Statistics charts for coordinate differences.

## 5 CONCLUSIONS

A flexible 3D modeling tool called floating models is proposed for model-based building reconstruction. Along with the *ad hoc* least-squares model-data fitting algorithm, building models can be reconstructed semi-automatically among versatile data sources. Horizontal parameters are fit from topographic maps and vertical parameters are fit from LiDAR data and DEM. According to the case study, the MBBR procedure goes smoother and faster with the increasing of operating experiences. Some characteristics of the proposed approach could be remarked:

1. For most of the normal buildings, floating model does increase efficiency than point-by-point measurement.
2. The labor-consuming measurement is carried out by computer while the operator only has to select model type and approximately fit it.
3. The inner constraints guarantees the geometric nature unchanged after reconstruction.
4. It is possible to reconstruct the whole building even if a part of it is occluded.
5. Floating models achieve similar accuracy as conventional photogrammetric measurements.
6. Although we fit model to versatile data sources in this research, floating model is also applicable to single data source, such as aerial photos.

However, the proposed three model types are not sufficient for dealing with every kind of buildings. To improve the completeness rate of MBBR, we recommend increasing the model types, such as cylinder, dome, slope-roof house, and ridge-roof house *etc.* If some pattern recognition techniques can be applied to detect the building model

type, the automation of MBBR may be greatly improved. The topology and the combination rules among models are also worth for further studying to make MBBR more robust and applicable.

## ACKNOWLEDGEMENT

The corresponding author is currently studying on further researches at the University of Calgary under the grant support (NSC97-2917-I-564-122) from the National Science Council, Republic of China (Taiwan). The authors would also like to show gratitude to the Ministry of Interior, Republic of China (Taiwan) for the support of the predecessor of this project, and the Taipei City Government for providing the digital topographic maps, digital aerial images and DEM, and Prof. L.C. Chen and his research team at the National Central University for their excellence collaboration. The photogrammetric assistances from the CECI Engineering Consultants Inc., Taiwan is highly appreciated.

## REFERENCES

- Ameri, B., 2000. Feature Based Model Verification (FBMV): A New Concept for Hypothesis Validation in Building Reconstruction. *The XIX<sup>th</sup> Congress of the International Society for Photogrammetry and Remote Sensing*, Amsterdam, Netherlands, pp. 24-35.
- Bhanu, B., D.E. Dudgeon, E.G. Zelnio, A. Rosenfeld, D. Casasent and I.S. Reed, 1997. Guest Editorial Introduction to the Special Issue on Automatic Target Detection and Recognition. *IEEE Transactions on Image Processing*, 6(1): 1-6.
- Böhm, J., C. Brenner, J. Gühring and D. Fritsch, 2000. Automated Extraction of Features from CAD Models for 3D Object Recognition. *The XIX<sup>th</sup> Congress of the International Society for Photogrammetry and Remote Sensing*, Amsterdam, Netherlands, pp. 76-83.
- Braun, C., T.H. Kolbe, F. Lang, W. Schickler, V. Steinhage, A.B. Cremers, W. Förstner and L. Plümer, 1995. Models for Photogrammetric Building Reconstruction. *Computers & Graphics*, 19(1): 109-118.
- Brenner, C., 1999. Interactive Modelling Tools for 3D Building Reconstruction. *Photogrammetric Week '99*. Wichmann, Stuttgart, pp. 23-34.
- Brenner, C., 2000. Towards Fully Automatic Generation of City Models. *The XIX<sup>th</sup> Congress of the International Society for Photogrammetry and Remote Sensing*, Amsterdam, pp. 85-92.
- Das, S., B. Bhanu and C.-C. Ho, 1996. Generic Object Recognition Using Multiple Representations. *Image and Vision Computing*, 4(5): 323-338.
- Englert, R. and E. Gülch, 1996. One-eye Stereo System for the Acquisition of Complex 3D Building Descriptions. *Geographic Information System*, 4: 1-11.
- Ermes, P., 2000. Constraints in CAD Models for Reverse Engineering Using Photogrammetry. *The XIX<sup>th</sup> Congress of the International Society for Photogrammetry and Remote Sensing*, Amsterdam, Netherlands, pp. 215-221.
- Grün, A., 2000. Semi-automated Approaches to Site Recording and Modeling. *The XIX<sup>th</sup> Congress of the International Society for Photogrammetry and Remote Sensing*, Amsterdam, Netherlands, pp. 309-318.
- Lang, F. and W. Förstner, 1996. 3D-City Modeling with a Digital One-eye Stereo System, *The XVIII<sup>th</sup> Congress of the International Society for Photogrammetry and Remote Sensing*, Vienna, Austria, pp. 415-420.
- Sester, M. and W. Förstner, 1989. Object Location Based on Uncertain Models, *Mustererkennung 1989*. Informatik Fachberichte 219. Springer Verlag, pp. 457-464.
- Tseng, Y.-H. and S. Wang, 2003. Semiautomated Building Extraction Based on CSG Model-Image Fitting. *Photogrammetric Engineering & Remote Sensing*, 69(2): 171-180.
- van den Heuvel, F.A., 2000. Trends in CAD-based Photogrammetric Measurement. *The XIX<sup>th</sup> Congress of the International Society for Photogrammetry and Remote Sensing*, Amsterdam, Netherlands, pp. 852-863.
- Vosselman, G. and H. Veldhuis, 1999. Mapping by Dragging and Fitting of Wire-Frame Models. *Photogrammetric Engineering & Remote Sensing*, 65(7): 769-776.
- Wang, S. and Y.-H. Tseng, 2009. Least-Squares Model-Image Fitting of Floating Models for Building Extraction from Images, *Journal of the Chinese Institute of Engineers*, 32(5).